

Reverse engineering adversarial attacks with fingerprints from adversarial examples

1st David Nicholson
Embedded Intelligence

Gaithersburg, MD, United States of America
david@embedintel.com

2nd Vincent Emanuele
Embedded Intelligence

Gaithersburg, MD, United States of America
vince@embedintel.com

Abstract—In spite of intense research efforts, deep neural networks remain vulnerable to adversarial examples: an input that forces the network to confidently produce incorrect outputs. Adversarial examples are typically generated by an attack algorithm that optimizes a perturbation added to a benign input. Many such algorithms have been developed. If it were possible to reverse engineer attack algorithms from adversarial examples, this could deter bad actors because of the possibility of attribution. Here we formulate reverse engineering as a supervised learning problem where the goal is to assign an adversarial example to a class that represents the algorithm and parameters used. To our knowledge it has not been previously shown whether this is even possible. We first test whether we can classify the perturbations added to images by attacks on undefended single-label image classification models. Taking a “fight fire with fire” approach, we leverage the sensitivity of deep neural networks to adversarial examples, training them to classify these perturbations. On a 17-class dataset (5 attacks, 4 bounded with 4 epsilon values each), we achieve an accuracy of 99.4% with a ResNet50 model trained on the perturbations. We then ask whether we can perform this task without access to the perturbations, obtaining an estimate of them with signal processing algorithms, an approach we call “fingerprinting”. We find the JPEG algorithm serves as a simple yet effective fingerprinter (85.05% accuracy), providing a strong baseline for future work. We discuss how our approach can be extended to attack agnostic, learnable fingerprints, and to open-world scenarios with unknown attacks.

Index Terms—deep neural network, adversarial machine learning, classification, supervised learning, adversarial examples

I. INTRODUCTION

Deep neural networks are susceptible to adversarial examples [1], [2]: inputs optimized to produce incorrect or unexpected outputs. Typically adversarial samples are generated by optimizing a perturbation δ added to a benign image x [3]. This added perturbation can be optimized by one of an ever-growing list of attack algorithms [4], [5], e.g., by maximizing the loss of the softmax function used to train single-label neural networks for image classification.

It remains unclear whether it will prove too computationally expensive or theoretically impossible [2], [6]–[11] to completely defend neural networks from adversarial attacks, at least for neural network models in their current mathematical

This material is based upon work supported by the Defense Advanced Research Projects Agency (DARPA) under Agreement No. HR00112090134. Approved for public release; distribution is unlimited.

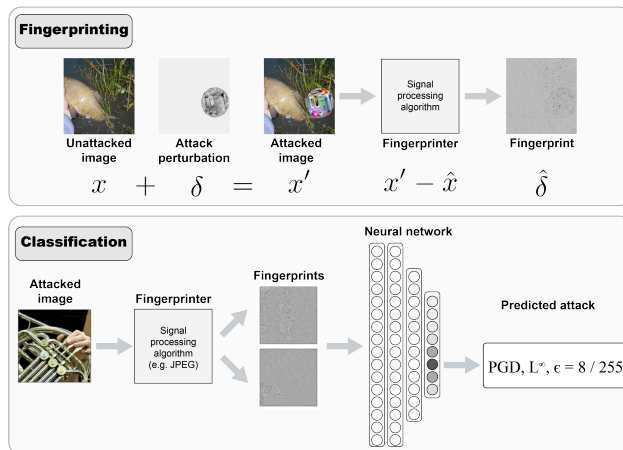


Fig. 1: Schematic of our approach to reverse engineering adversarial attacks. Top row illustrates “fingerprinting” adversarial examples to obtain an estimate of the perturbation δ added by an attack to an image. Bottom row illustrates training deep neural networks to classify fingerprints from adversarial examples, assigning each to a class that corresponds to an attack algorithm and parameters. Our goal in formulating the problem this way is to train models on large datasets of fingerprints from attacks generated with existing software frameworks, and then classify attacked images without knowledge of the attack or access to the perturbation, by using fingerprints.

formulation. Defenses are notoriously difficult to evaluate, in spite of concerted efforts by the community to establish good practices [12]. Given the difficulties faced in developing defenses against adversarial attacks, we consider a different question. We ask whether it is possible to reverse engineer adversarial attacks, using adversarial examples. If this were possible, it could deter bad actors from deploying adversarial example in the real world, e.g., due to the threat of attribution. Accordingly, we identified two capabilities that would be desirable in a system for classifying and searching datasets of adversarial examples. We describe these two capabilities then explain how we formulate a machine learning task that can produce models with those capabilities.

A. Classifying perturbations by attack

The first capability we would want such a system to have is to classify adversarial examples by the attack algorithm used to generate them. Of course it may be possible to reverse engineer attacks without classifying them, e.g., by literally “reversing” the optimization. In other words, here we formulate reverse engineering as a supervised classification problem. Our motivation is pragmatic. We ask whether we can leverage widely used and well understood methods, as well as software frameworks that have been developed to generate large datasets of adversarial examples, that we can use to train a machine learning model to classify by attack algorithm.

To the best of our knowledge, it is still an open question in the literature whether adversarial examples can be classified by attack algorithm. We emphasize that classifying examples by attack algorithm is different from detecting that an image has been attacked, e.g. by monitoring the outputs of the model for outliers, or (equivalently) classifying an image as an adversarial example [13].

It could be the case that very different attack algorithms all arrive at similar perturbations, in which case it would be difficult or impossible to classify them. For example, a PGD attack with an L^∞ bound of $\epsilon=8/255$ on a specific instance of a ResNet50 model may produce perturbations that are indistinguishable from those produced by a Square attack with the same bound, on the same model. Alternatively, it could be the case that, because of the abundance of adversarial examples in image space, each algorithm can produce unique perturbations that other attacks are much less likely to find. By the same token, it could be the case that classifying adversarial examples by attack algorithm can be done using the attacked images themselves, and therefore is trivial. Alternatively, classification of attacks might require the perturbation added by an attacker, which a defender may not have access to, even when they know the image is attacked. These open questions make it important to carry out a rigorous study of whether or not this task is even possible.

1) *Classifying families of adversarial attacks:* A related question that arises when considering how to reverse engineer adversarial attacks is whether this problem is hierarchical. Can attacks be grouped somehow, and could this grouping help with classification? In this work we again operationally define families of attacks with the goal of understanding how this relates to our ability to classify them. For brevity we avoid summarizing the history of adversarial attacks, and refer the reader to recent reviews. These reviews show that attacks can be schematized in several ways [4], [5], and grouped along several dimensions. Although it is important to consider all dimensions, in our studies we focus on two: the *threat model*, and the *constraint*. Researchers in this area often speak of a *threat model*, a term that summarizes the access that an attacker has to the machine learning model. Under a *white-box* threat model, the attacker has total access, and thus can compute the gradient, which generally speaking allows for more powerful attacks. In contrast, under a *black-box*

threat model, the attacker only has access to outputs of the machine learning model, which may be a single predicted label or a vector of scores. Black-box attacks generally require many more queries or iterations to produce a powerful attack. Another dimension along which attacks can be grouped is the constraints placed on the perturbation. It is common for both white-box and black-box attacks to use L^p -ball constraints, where the size of a perturbation generated by an attack is constrained to be less than some ϵ as computed with the corresponding p -norm (e.g., an L^2 norm). In contrast, patch attacks do not constrain the perturbation size but constrain the attack to a confined space within the image [14]. Considering just these two dimensions, we can already begin to group each attack algorithm into a family. E.g., both Fast Gradient Sign Method (FGSM) [2] and Projected Gradient Descent (PGD) [3], could be considered part of a family of white-box, L^p -ball attacks, while square attack [15] could be considered part of the family of black-box, L^p -ball attacks. We of course recognize that attacks can be grouped in other ways —e.g., one might consider a patch attack a physical attack on real-world objects, as opposed to white-box attacks on images [16]— but we think most researchers would not find it controversial to group attacks into families, and agree that it would be useful to ask whether the ability to classify adversarial examples depends in part on the family. An effect of family figures into our analyses below.

B. Estimating perturbations in an attack-agnostic manner

Assume for a moment that we can classify adversarial examples by attack algorithm, but that this is best done using the perturbation added by the attack, not the attacked image itself (as our result below indicate). This suggests that the second capability we will want our system to have is to estimate the true perturbation δ generated by an attack, ideally in an attack-agnostic fashion that does not require us to develop a reverse engineering method for each algorithm or family of attacks. Here again, little work has been done, and so we take a methodical approach. As we detail in Section II, we test whether we can obtain estimates of the perturbations using familiar signal-processing methods for image compression and restoration, namely the JPEG algorithm and a compressed sensing-based image reconstruction algorithm. We were first motivated to take this approach after observing that simply reconstructing attacked images \mathbf{x}' and subtracting the reconstruction $\hat{\mathbf{x}}$ from \mathbf{x}' to obtain an estimate of the perturbation $\hat{\delta}$ can produce a mark that is obvious upon visual inspection. We show an example in the top panel of Figure 1. We refer to the estimates of $\hat{\delta}$ so obtained as “fingerprints”. Our motivation for this approach also springs from previous work showing that such algorithms can remove the perturbation δ added by an attacker [17]. We are of course aware of work showing that adaptive attacks can produce perturbations that successfully attack models even after input transformations such as JPEG are applied [18]. Our express goal here is *not* to defend the model, but to obtain an estimate of the perturbation in an attack-agnostic fashion. We see the simplifying assumption

of testing on undefended models as part of our methodical approach, and consider it important to test in this simplified setting to lay the foundation for future work.

C. Our contribution

Without a theory of adversarial examples, we cannot state unequivocally that each capability can be designed, but we can test whether each is possible empirically. Here we provide evidence that such a system can be designed with the two capabilities just described, suggesting it will be possible to reverse engineer adversarial attacks. Our contributions are as follows:

- We show that given the true perturbations δ added to benign images, we can predict with near perfect accuracy the attack used and at least one of its parameters, the value of the bound ϵ for bounded attacks.
- We then show that we can obtain estimates of the perturbation, which we call fingerprints, in an attack agnostic manner that still allows us to classify the perturbations according to attack.
- We demonstrate that fingerprints obtained with simple signal processing methods allow us to classify attacks with accuracy of 84.49%. Compared to our empirical upper bound of near 100% accuracy shown with true perturbations, this leaves room for improvement, but we provide a strong baseline for future work using data-driven methods, a point we return to in the discussion.

II. APPROACH

A. Notation

To discuss our method, we adopt the following notation: Let F_θ be a deep neural network model with parameters θ trained to map inputs \mathbf{x} to a set of c class labels $Y = \{y_1, y_2, \dots, y_c\}$. For all supervised learning problems, we update θ by minimizing a loss function L .

Where needed, we use a superscript F_θ^δ to distinguish a deep neural network trained to classify adversarial examples into attack classes $Y^\delta = \{y_1, y_2, \dots, y_c\}$ from the standard network for single-label image classification F_θ . For such a network F_θ^δ , each class c in Y is a specific attack algorithm from one of the families we study, where the class also denotes a bound and an epsilon parameter when the attack uses such constraints: e.g., the PGD attack from the white-box L^p -ball family, with an L^∞ bound and $\epsilon = 4/255$. (We define these further below.) Using $\hat{\delta}$ as a superscript denotes that we have trained F_θ^δ on some estimate of the perturbation δ added by an attack to an image \mathbf{x} to produce the adversarial example \mathbf{x}' . We call these estimates $\hat{\delta}$ “fingerprints”.

B. Classifying adversarial images by attack algorithm

Here we focus on attacks on deep neural network models for single-label image classification, as this is where much of the research on attacks has centered. To simplify the problem, we assume that attacked models are undefended, and that a researcher is able to train machine learning models on datasets of attacked images without threat of adversarial

Attack algorithm	Attack family	ϵ values	Other parameters
FGSM	White box, L^p -ball	{1, 2, 4, 8} / 255	None
PGD, L^∞	White box, L^p -ball	{1, 2, 4, 8} / 255	250 steps, step size = $(2.5 * \epsilon)$ / steps
PGD, L^2	White-box, L^p -ball	{0.25, 0.5, 1.0, 2.0}	250 steps, step size = $(2.5 * \epsilon)$ / steps
Square, L^∞	Black box, L^p -ball	{1, 2, 4, 8} / 255	10k queries
Universal patch	Patch attack	None	None

TABLE I: Attack algorithms, families, and parameters used.

attack. Taking a “fight fire with fire” approach, we train neural networks to classify adversarial examples by the attack used to optimize the perturbation δ added to the benign image \mathbf{x} . This approach is motivated by previous work showing that deep neural networks are susceptible to adversarial examples in part because they latch on to high-frequency components of images that are largely imperceptible to humans [19]–[21].

C. Adversarial attacks

1) *Attack families, algorithms, and parameters:* Although research on adversarial attacks is rapidly evolving, the community of researchers has recognized families of attacks. As stated in Section II, we group attack algorithms into three families for our problem formulation: white box L^p -ball attacks, black box L^p -ball attacks, and patch attacks. We see this is a reasonable choice given that much work has focused on attacks from these three families.

As shown in Table I, we generated attacks with two algorithms from the white box family, FGSM [2] and PGD [3], and one each from the black box and patch families: square attack [15] and the universal patch attack of [14], respectively. For purposes of classification, we further divided attacks by the value of p used for the L^p norm, (i.e., L^2 or L^∞) and the value of the bound parameter ϵ , where we used 4 unique values per attack and norm. In total this gave us 17 different classes, as shown in Table I.

2) *Dataset:* All attacks were generated on images from Imagenette¹, a version of the ImageNet dataset with only 10 classes, and approximately 2000 images per class. We preserved the training and test sets from Imagenette to avoid contaminating our test set with training images, as explained further below. Thus, we generated attacked images for both the training and test sets. For all experiments here, we used only successful attacks. The number of attacked images thus generated for each combination of attack and epsilon size (for bounded attacks) ranged from 5750-6700 for the training set, and from 2400-2990 for the validation set.

D. Taking “fingerprints” of perturbations

After generating these pools of attacked images, we “took fingerprints” from them. The same pipeline was used for all

¹<https://github.com/fastai/imagenette>

combinations of fingerprint methods and parameter settings reported.

To extract fingerprints from attacked images, we used different methods for image compression and reconstruction, under the working hypothesis that these methods will tend to remove the adversarial perturbation added to an image. If this hypothesis is true, then we should be able to subtract the reconstructed image \hat{x} from the attacked image x to obtain an estimate of the perturbation $\hat{\delta}$ added by an attacker. Using this notation, for all reconstruction methods, we obtain our fingerprint like so:

$$\hat{\delta} = x' - \hat{x}$$

a) *JPEG*: To use JPEG as a fingerprint extraction technique, we simply set the quality parameter of JPEG and then used the compressed image x_{jpeg} to create a fingerprint $\delta_{jpeg} = x' - x_{jpeg}$.

b) *Compressed sensing*: At a high level, compressed sensing is a family of algorithms that obtains high-fidelity estimates of a signal given many fewer samples than required by classical signal processing theorems, by solving an undetermined system of linear equations with a sparsity constraint. The system of equations typically consists of a random sampling matrix S , a dictionary D that transforms the signal into a domain where it can be considered sparse (e.g., DCT), and a regularization constant λ that enforces sparsity. The algorithm we use also adds a k/n parameter, the ratio of random samples to the number of true samples in the signal (for images, the percentage of pixels). By randomly grabbing a subset of samples, in effect we use a Bernoulli sampling matrix.

Given this set of parameters for compressed sensing, $(S, D, k/n, \lambda)$, we solve for the attack fingerprint δ_{cs} as

$$\chi_{cs} = \left\{ \chi \in \mathbb{R}^n \mid \min_{\chi} \|b - SD\chi\|_2 + \lambda \|\chi\|_1 \right\} \quad (1)$$

$$x_{cs} = D\chi_{cs} \quad (2)$$

$$\delta_{cs} = x' - x_{cs}. \quad (3)$$

1 is typically solved using techniques described in [22].

E. Neural network training

1) *Dataset preparation*: We built training and test sets from our database of fingerprints to train and test neural network models F_{θ}^{δ} that assign labels to adversarial examples according to attack class. So that we could avoid contaminating the test set with the training set, we maintained the original splits from Imagenette. That is, we built our training sets using fingerprints extracted from attacked images generated with the Imagenette training set, and likewise built our test sets with fingerprints extracted from attacked images generated with the Imagenette test set. Both our training and test sets contained fingerprints taken from 1000 unique images from the original Imagenette dataset. These unique images were sampled randomly when creating the splits from the larger pools of fingerprints generated as described above. The training set was

further split into training and validation sets, with 90 percent of the samples used for training, and the other 10 percent used to validate performance during training. Before creating splits as just described, we filtered the total set of adversarial examples to keep only successful attacks. For the 17-class dataset used for our main result, this gave us a training set size of 124156 samples and a test set size of 52283 samples, for each fingerprint or other input used to train networks (the true perturbation δ or the adversarial example itself). (I.e., there was a training set of 124156 adversarial examples, and a separate training set of 124156 JPEG reconstructions, etc.)

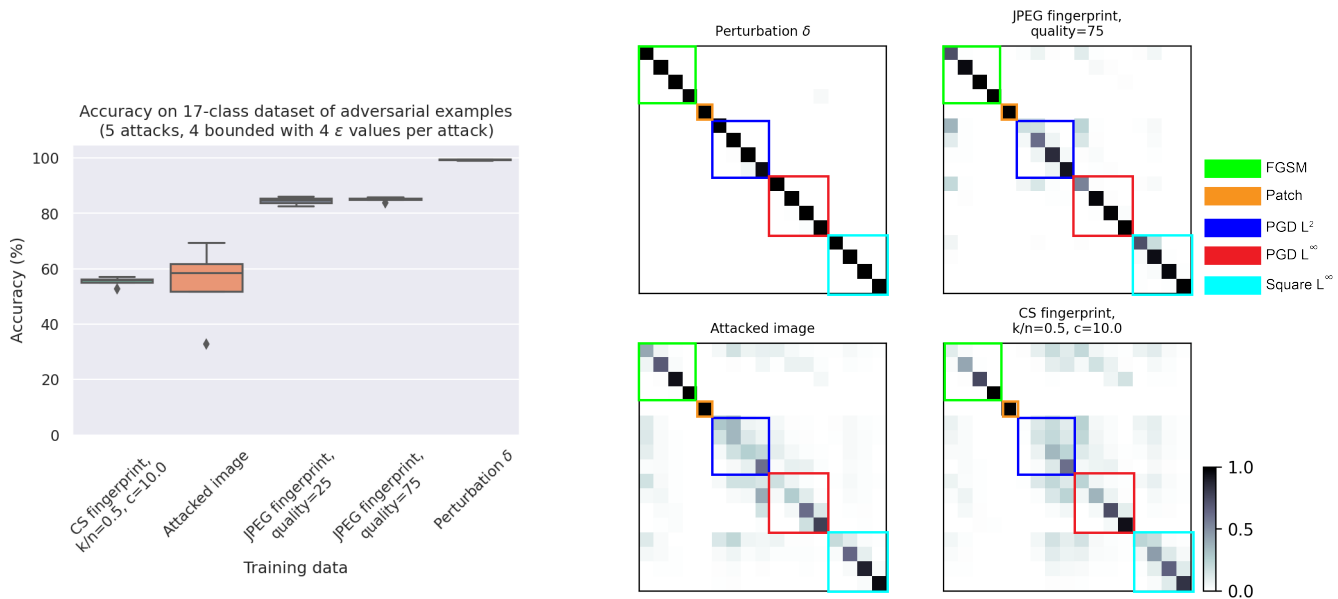
2) *Model, optimizer, hyperparameters*: For all experiments using fingerprints or comparison training data, we used the ResNet50 architecture [23] as the neural network model F_{θ}^{δ} . As our loss function L we used standard cross-entropy loss, and we optimized parameters with the Adam optimizer [24] with the learning rate $\alpha = 0.01$, and a batch size of 128. We configured training such that networks would train for a maximum of 50 epochs (where each epoch is an iteration through the entire training set), but used an early stopping scheme. Early stopping depended on accuracy as measured on the validation set every 400 steps (i.e., every 400 batches). If four validation checkpoints elapsed without accuracy increasing beyond the maximum recorded, then training stopped. This meant that in practice the optimization rarely ran for the full 50 epochs. Visually inspecting the training histories showed that this scheme enabled sufficient training for the optimization to converge while preventing networks from overfitting on the training set. For all experiments, we trained four replicates of ResNet50, where each replicate had weights initialized before training.

III. RESULTS

A. Classification of adversarial examples by attack algorithm

We began by asking whether it is even possible to classify adversarial examples by the attack algorithm and parameters used. As stated in Section I, we start here because we formulate reverse engineering attacks as a supervised learning problem, and because to our knowledge this remains an unaddressed question in the literature. To answer this question, we began by training a ResNet50 on the perturbations added to images from the 10-class Imagenette dataset, by attacking a separate, undefended ResNet50 model pre-trained on all of ImageNet. We generated adversarial examples with 5 different attacks, 4 of them bounded, with 4 epsilon values per attack (see Section II), giving us us a 17-class dataset. Results are shown in Figure 2

We found that, yes, we were able to assign labels to perturbations corresponding to the attack algorithm and size of the epsilon bound on attacks, as shown in the rightmost column of Figure 2a. The ResNet50 trained on the perturbations alone was able to perform this task with near-perfect accuracy: $99.4\% \pm 0.15\%$ (mean \pm standard deviation) across 4 training replicates (instances of a model trained from randomly initialized weights). In contrast, when we asked the same ResNet50 model to perform the same task given the attacked images



(a) Accuracy of ResNet50 models trained to classify adversarial examples according to attack class. Box and whisker plots show distribution of accuracies across four training replicates. X-axis indicates type of data that models were trained to classify: either the perturbation δ added by an attack to an image, the attacked image itself, or a "fingerprint", an estimate of δ obtained with a signal processing algorithm.

(b) Confusion matrices for ResNet50 models, where rows are ground truth labels, columns are predicted labels, and grayscale intensity in each square indicates probability of predicting each label, normalized within rows. Colored rectangles indicate attack algorithms. ϵ values are sorted within attack algorithm to increase from top to bottom and from left to right. Each plot is generated from predictions of one training replicate of a ResNet50 model. In general, results were similar across replicates and so a representative example is shown.

Fig. 2: Results of training deep neural networks to assign attack classes to adversarial examples

themselves (i.e., the benign image x + the perturbation δ we classified before), we were only able to achieve $54.84\% \pm 15.62\%$ accuracy on the held-out test set (Figure 2a, second column from left). We analyze these two results further below, but note that taken together they indicate that it is possible to classify perturbations by attack algorithm and parameters, given the true perturbation, and additionally suggest that it will not be sufficient to simply classify the attacked images themselves.

B. Obtaining and classifying estimates of perturbations by fingerprinting with signal-processing methods

Given this initial evidence that it is possible to classify perturbations by attack and parameters used, we next asked whether we would be able to classify attacks even if we did not have access to the true perturbations. This would be the case if we detected that the image was attacked, by inspecting the image and comparing the human label with the incorrect outputs of an image-classification model, but we did not have knowledge of the attack used. In this situation, we would somehow need to obtain an estimate of the perturbation added by an attacker.

Motivated by previous work on defenses showing signal processing algorithms for image compression and reconstruction can remove perturbations added by non-adaptive adversarial attacks, we chose to test two of these algorithms as

methods for obtaining estimates of the perturbation δ added to attacked images, as detailed in Section II.

We began by testing with the JPEG algorithm. We trained ResNet50 models on "fingerprints" produced by first compressing and then decompressing the attacked images with JPEG, treating this as an estimate of the benign image before attack \hat{x} that we subtracted from the attacked image x to give us an estimate of the perturbation added by the attack, $\hat{\delta}$. To test for any effect of JPEG parameters, we generated these "fingerprints" with a quality parameter of 75, as used in the original paper proposing JPEG as a defense [17], and also with quality=25. ResNet50 models trained on JPEG quality=75 achieved an accuracy of $85.05\% \pm 0.83\%$ and those trained on JPEG quality=25 achieved an accuracy of $84.49\% \pm 1.46\%$. By comparison, models trained on compressed sensing (CS) fingerprints achieved $55.39\% \pm 1.87\%$ accuracy. These results are also shown in the middle columns of Figure 2a.

To better understand these results, we generated confusion matrices for each of the models, and visually inspected these to see if they provided additional insights. These are shown in Figure 2b. The first thing we noticed when inspecting these plots was the inverse relationship between the size of the epsilon bound and the size of the error. I.e., attacks generated with smaller epsilon bounds were more difficult to classify. Additionally we observed that attacks with an L^∞ bound appeared to be easier to classify; results were consistent for these attacks except for the smallest epsilon values, whereas

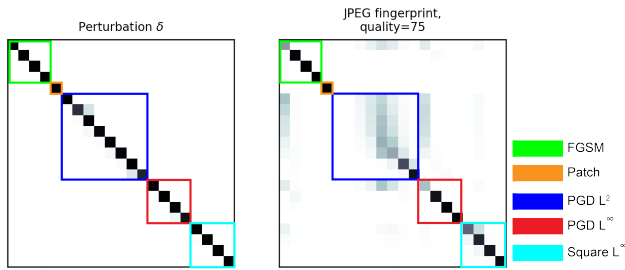


Fig. 3: Confusion matrices for ResNet50 models trained on dataset with more ϵ values for PGD- L^2 attack. As in Figure 2b, rows are ground truth labels, columns are predicted labels, and grayscale intensity in each square indicates probability of predicting each label, normalized within rows. Colored rectangles indicate attack algorithms. ϵ values are sorted within attack algorithm to increase from top to bottom and from left to right. Each plot is generated from predictions of one training replicate of a ResNet50 model. In general, results were similar across replicates and so a representative example is shown.

the networks tended to make more mistakes for the PGD L^2 attacks.

C. Performance when adding more, smaller ϵ values

Because we noted that our purely supervised classification approach was challenged by smaller values of ϵ , as can be seen in the confusion matrices in 2b, and because PGD L^2 attacks in particular appeared to be challenging to classify, we chose to push on this result further. We generated additional PGD- L^2 attacks with another set of values: 0.1, 0.2, 0.3 and 0.4, and then used this expanded dataset to repeat the experiments where we trained ResNet50 models to classify the true perturbation δ and the JPEG-based fingerprints.

Again we saw that when given the true perturbation δ , networks could classify this expanded dataset quite well, achieving $97.18\% \pm 1.96\%$ accuracy. In contrast, we saw a drop in accuracy for models trained on JPEG fingerprints (quality=75), from $85.05\% \pm 0.83\%$ we saw before to $72.11\% \pm 1.65\%$ on this expanded dataset with more ϵ values that were “closer” to each other. We generated confusion matrices for these models and indeed saw that for the PGD- L^2 class, the models trained on JPEG fingerprints tended to misclassify all but those from attacks generated using the largest ϵ values. These confusion matrices are shown in Figure 3.

Taken together, our results provide positive evidence that it is possible to classify adversarial examples according to attack algorithm, but that a purely supervised approach may be challenged when faced with the task of estimating continuous parameters like the value of ϵ bound used with an attack.

D. Additional analysis

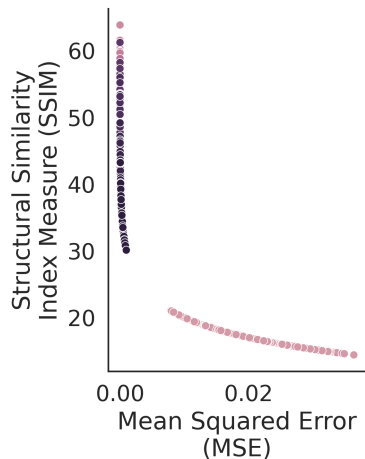
Finally, we carried out additional analyses to test possible alternate explanations for our results.

1) *Image quality*: First we asked whether different attacks might have different effects on image quality. If so, this could serve as a form of data leakage, where the network simply learns to classify an image by the amount of noise in it. To test for this possibility, we generated 2-D plots of the mean square error (MSE) versus the structural similarity index metric (SSIM) for each attacked image, compared to the benign image before attack, as shown in Figure 4a. SSIM declined exponentially as MSE increased, which is perhaps not surprising, but we note that these metrics are not necessarily tightly linked; SSIM was specifically designed as a sensitive perceptual measure that detects changes in image quality that MSE does not take into account, while MSE can increase greatly even due to changes that the human eye would not detect (e.g. shifting the entire image one pixel in one direction) [25]. The important thing to notice here is that we did not see any obvious clustering of attack according to these two values. While this does not let us rule out the possibility of data pollution by image quality, we felt such an explanation was less likely given this result, and so we moved on to consider another possible explanation.

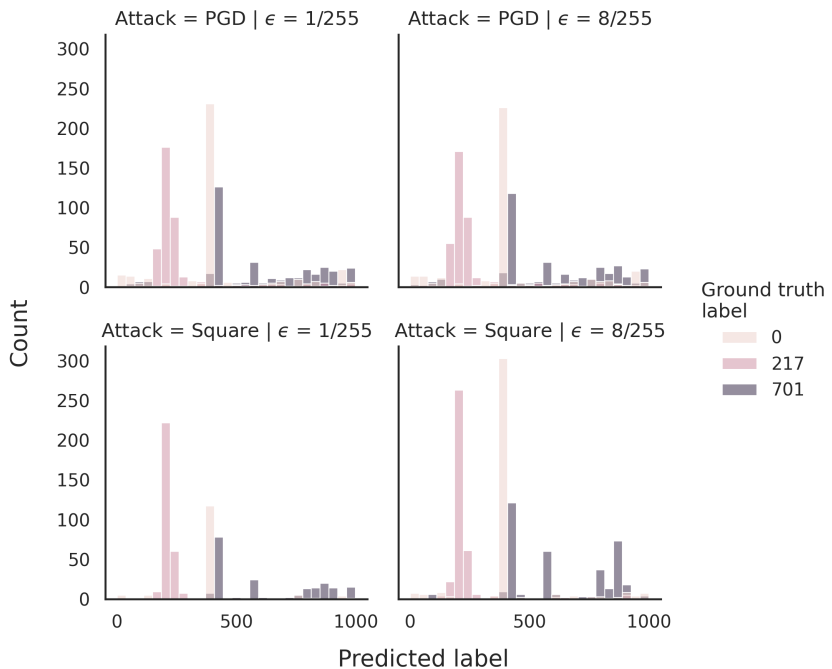
2) *Distribution of class labels produced by untargeted attacks*: A second alternative explanation we considered was that different attacks might consistently generate specific labels for untargeted attacks, and this could provide a shortcut that the network would learn. I.e., an untargeted PGD- L^∞ attack with $\epsilon = 4$ might tend to convert the “fish” class into “airplane”, whereas the untargeted Square- L^∞ attack might tend to convert the same “fish” class into “truck”. To test for this possibility, we plotted the distribution of targeted labels produced by each attack for PGD- L^∞ and Square- L^∞ , for all classes and all epsilon sizes. In Figure 4b we show these results. For readability, the distribution for only three classes is shown. This analysis did not produce evidence suggesting that different attacks produce different distributions of labels that a model might be able to learn. In fact, we observed the opposite, the distributions appear to be quite similar across attack types and across ϵ values. For example, in the upper left panel, the PGD- L^∞ attack was most likely to convert images with ground truth label 0 (“tench”) to label 389. This was the case in all other panels as well, and for all other classes, although it was also clear that the label distributions produced by attacks on some classes were higher entropy than others (compare for example the distributions produced for class “0” with the distributions for class “701” shown in Figure 4b). This result suggests that the distributions of labels generated by attacks are largely a function of the decision boundaries learned by the model under attack, consistent with previous work [2], [6], and strengthens our claim that deep neural networks trained on the perturbations or fingerprints are learning to classify the attacks and epsilon sizes, not the targeted label, since the latter can vary highly within a ground truth class.

IV. DISCUSSION

We investigated whether it is possible to reverse engineer attacks, in part because of the difficulties faced in develop-



(a) Mean Squared Error (MSE) vs Structural Similarity Index Metric (SSIM). Hue indicates attack class label. Measurements are taken from attacked images, in comparison with original benign images.



(b) Distribution of labels produced by untargeted attacks. Distributions of predicted labels are shown for three ground truth classes, for two different attacks (rows) and two different ϵ values (columns)

Fig. 4: Analysis of classification results

ing defenses against them. More specifically, we formulated reverse engineering as a problem of classification with supervised learning methods. We found that we were able to classify adversarial examples according to the attack algorithm and the size of the epsilon bound used, given the true perturbation added to the attack. Classifying the attacked images themselves was not sufficient, although we observed that it was possible for attacks with large perturbations (e.g., large values of the bound ϵ for bounded attacks). Additionally, we tested whether we could “fingerprint” attacked images to obtain an estimate of the perturbations added by attack algorithms. We showed that the well established and widely available JPEG algorithm can be used to provide a good estimate of the perturbation added by a wide range of attacks, and that neural network models trained on these fingerprints achieved $\sim 85\%$ accuracy.

These results are not without caveats. Our study focuses on reducing the problem to its simplest form, and so we have not for example tested our approach on adaptive adversarial attacks, and we have not tested whether we can modify adaptive attacks to render the task of classifying adversarial examples difficult. In spite of these limitations, the results presented here are still important, directly demonstrating for the first time that classifying perturbations according to attack is possible, and providing a strong baseline for future work for more sophisticated methods of reverse engineering attacks.

A. Future work

We identify several directions that future studies can take based on our results. The first would be to combine classification with regression to better estimate parameters such as the value of ϵ used as a bound. As we observed, deep neural network models are quite capable of classifying attack algorithms given the true perturbation, but it is more difficult to classify the values of parameters such as ϵ . A method to achieve both might be to combine classification with a regression loss, in the same way that object detection models apply classification loss to the labels predicted for bounding boxes and regression loss to the coordinates of the bounding box. This would allow for prediction of the continuous variable of the epsilon bound and could be extended to other parameters such as the number of steps.

Our results on fingerprints also make a strong case for a learnable, attack-agnostic method for estimating the perturbation δ . This data-driven approach may seem obvious to researchers with a deep learning mindset, but the clear differences we observed between signal processing algorithms suggest that careful study may incorporate appropriate biases or constraints into fingerprinting models that improve performance. In particular the superior performance of JPEG compared to compressed sensing suggests that a neural network model for estimating fingerprints may benefit from integrating the perceptual components of the JPEG algorithm into its architecture. Previous work has shown that the JPEG algorithm can be implemented as a neural network [26], and recent

studies of adversarial attacks have suggested that algorithms tend to place energy in specific channels of the color space used by the JPEG algorithm [27], [28].

A last consideration for future studies will be how to deal with unknown attacks that are not contained within the dataset. This would need to be studied with open-world and open-set classification problem formulations. A natural starting point would be modified loss functions such as the entropic loss proposed by [29]. Note that the derivation of the entropic loss assumes a neural network with a fully connected layer without a bias term just before the final output layer, which may limit its applicability with state-of-the-art neural network models for single-label image classification such as ResNet, although practically speaking one can just add such a layer to a ResNet model as [29] do in their experiments.

V. CONCLUSION

We have shown that the exquisite sensitivity of deep neural networks to adversarial examples can be converted from a bug into a feature. Our results are consistent with the idea that deep neural network models can classify adversarial examples according to attack algorithm. These findings set the stage for future work on reverse engineering adversarial attacks.

REFERENCES

- [1] C. Szegedy, W. Zaremba, I. Sutskever, J. Bruna, D. Erhan, I. Goodfellow, and R. Fergus, "Intriguing properties of neural networks," *arXiv:1312.6199 [cs]*, Feb. 2014.
- [2] I. J. Goodfellow, J. Shlens, and C. Szegedy, "Explaining and Harnessing Adversarial Examples," *arXiv:1412.6572 [cs, stat]*, Mar. 2015.
- [3] A. Madry, A. Makelov, L. Schmidt, D. Tsipras, and A. Vladu, "Towards Deep Learning Models Resistant to Adversarial Attacks," *arXiv:1706.06083 [cs, stat]*, Sep. 2019.
- [4] E. Tabassi, K. J. Burns, M. Hadjimichael, A. D. Molina-Markham, and J. T. Sexton, "A taxonomy and terminology of adversarial machine learning," Preprint, Oct. 2019.
- [5] N. Akhtar, A. Mian, N. Kardan, and M. Shah, "Advances in Adversarial Attacks and Defenses in Computer Vision: A Survey," *IEEE Access*, vol. 9, pp. 155 161–155 196, 2021.
- [6] D. Warde-Farley and I. Goodfellow, "11 adversarial perturbations of deep neural networks," *Perturbations, Optimization, and Statistics*, vol. 311, 2016.
- [7] T. Tanay and L. Griffin, "A Boundary Tilting Perspective on the Phenomenon of Adversarial Examples," *arXiv:1608.07690 [cs, stat]*, Aug. 2016.
- [8] A. Shafahi, W. R. Huang, C. Studer, S. Feizi, and T. Goldstein, "Are adversarial examples inevitable?" Feb. 2020.
- [9] Y. Yang, R. Khanna, Y. Yu, A. Gholami, K. Keutzer, J. E. Gonzalez, K. Ramchandran, and M. W. Mahoney, "Boundary thickness and robustness in learning models," *arXiv:2007.05086 [cs, stat]*, Jan. 2021.
- [10] Z. Dai and D. K. Gifford, "Image classifiers can not be made robust to small perturbations," *arXiv:2112.04033 [cs, stat]*, Dec. 2021.
- [11] R. Yousefzadeh, "Decision boundaries and convex hulls in the feature space that deep learning functions learn from images," *arXiv:2202.04052 [cs, math]*, Feb. 2022.
- [12] N. Carlini, A. Athalye, N. Papernot, W. Brendel, J. Rauber, D. Tsipras, I. Goodfellow, A. Madry, and A. Kurakin, "On Evaluating Adversarial Robustness," *arXiv:1902.06705 [cs, stat]*, Feb. 2019.
- [13] N. Carlini and D. Wagner, "Adversarial Examples Are Not Easily Detected: Bypassing Ten Detection Methods," *arXiv:1705.07263 [cs]*, Nov. 2017.
- [14] T. B. Brown, D. Mané, A. Roy, M. Abadi, and J. Gilmer, "Adversarial patch," *arXiv preprint arXiv:1712.09665*, 2017.
- [15] M. Andriushchenko, F. Croce, N. Flammarion, and M. Hein, "Square Attack: A query-efficient black-box adversarial attack via random search," *arXiv:1912.00049 [cs, stat]*, Jul. 2020.
- [16] N. Akhtar and A. Mian, "Threat of Adversarial Attacks on Deep Learning in Computer Vision: A Survey," *IEEE Access*, vol. 6, pp. 14 410–14 430, 2018.
- [17] C. Guo, M. Rana, M. Cisse, and L. van der Maaten, "Countering Adversarial Images using Input Transformations," *arXiv:1711.00117 [cs]*, Jan. 2018.
- [18] R. Shin and D. Song, "Jpeg-resistant adversarial images," in *NIPS 2017 Workshop on Machine Learning and Computer Security*, vol. 1, 2017.
- [19] H. Wang, X. Wu, Z. Huang, and E. P. Xing, "High-Frequency Component Helps Explain the Generalization of Convolutional Neural Networks," in *2020 IEEE/CVF Conference on Computer Vision and Pattern Recognition (CVPR)*. Seattle, WA, USA: IEEE, Jun. 2020, pp. 8681–8691.
- [20] D. Yin, R. G. Lopes, J. Shlens, E. D. Cubuk, and J. Gilmer, "A Fourier Perspective on Model Robustness in Computer Vision," *arXiv:1906.08988 [cs, stat]*, Sep. 2020.
- [21] C. Zhang, P. Benz, A. Karjauv, and I. S. Kweon, "Universal Adversarial Perturbations Through the Lens of Deep Steganography: Towards A Fourier Perspective," *arXiv:2102.06479 [cs]*, Feb. 2021.
- [22] S. Tao, D. Boley, and S. Zhang, "Local linear convergence of ISTA and FISTA on the LASSO problem," *SIAM Journal on Optimization*, vol. 26, no. 1, pp. 313–336, 2016.
- [23] K. He, X. Zhang, S. Ren, and J. Sun, "Deep residual learning for image recognition," 2015.
- [24] D. P. Kingma and J. Ba, "Adam: A method for stochastic optimization," *arXiv preprint arXiv:1412.6980*, 2014.
- [25] Z. Wang and A. C. Bovik, "Mean squared error: Love it or leave it? A new look at Signal Fidelity Measures," *IEEE Signal Processing Magazine*, vol. 26, no. 1, pp. 98–117, Jan. 2009.
- [26] R. Shin and D. Song, "JPEG-resistant Adversarial Images," p. 6.
- [27] C. Pestana, N. Akhtar, W. Liu, D. Glance, and A. Mian, "Adversarial perturbations prevail in the y-channel of the ycbcr color space," *arXiv preprint arXiv:2003.00883*, 2020.
- [28] —, "Adversarial Attacks and Defense on Deep Learning Classification Models using Y C b C r Color Images," in *2021 International Joint Conference on Neural Networks (IJCNN)*. IEEE, 2021, pp. 1–9.
- [29] A. R. Dharmija, M. Günther, and T. E. Boult, "Reducing Network Agnostophobia," *arXiv:1811.04110 [cs]*, Dec. 2018.